UNIVERSITAT DE BARCELONA
Departament d'Astronomia i Meteorologia

UNIVERSITAT DE BARCELONA

Determination of the distance to the Andromeda Galaxy using variable stars

Memòria presentada per
Francesc Vilardell Sallés
per optar al grau de
Doctor en Física

Barcelona, gener de 2009

A Large optical flare*

The analysis of the time series of the variable stars in our photometric catalog (Chap 2) revealed a large optical flare event on 2000 September 25. Flares are known as sudden and violent events releasing magnetic energy and hot plasma from the stellar atmospheres (see Sect. A.1). The analysis of the observed phenomenon is presented as an example of the potential of our photometric catalog for further studies. The high quality of the obtained photometry and the good time sampling allowed the estimation of the stellar properties (Sect. A.2), an accurate characterization of the main flare (Sect. A.3) and several minor events (Sect. A.4).

A.1 The observed phenomenon

Flares are observed on magnetically active stars and, much more closely, on the Sun. Electromagnetic radiation is emitted across the entire spectrum, from radio waves through the optical range to X-rays and γ-rays. The total energy released during a typical solar flare is in the order of 10^{30} erg, while the largest solar two-ribbon flares can emit up to 10^{32} erg.

According to the accepted model of solar flares, in the upper atmosphere, between oppositely oriented magnetic field lines, a current sheet forms and magnetic reconnection takes place, which results in acceleration of particles, and thus produces electromagnetic radiation and plasma heating. On the basis of the solar paradigm one could simply expect that modeling stellar flares is just a question of scaling (e.g., as a function of the released energy, size, duration, etc.). However, besides general similarities, stellar flare observations also unveil problems that cannot be explained with the extended canonical solar flare model, arising from the different spectral distribution of the emitted energy, the role of age and spectral type of the host star, the multiform magnetic field topologies on stars, the tidal forces in active binaries, etc. The only way we could get closer to drawing

*The contents of this chapter were published in Kovári et al. (2007).

up similarities and differences between solar and stellar flares is to continuously broaden the ensemble of analyzed flares (solar and stellar as well), thus making an observational base of different types of flaring activities available for theoretical purposes. This is how solar flare observations can help in the correct interpretation of stellar flares, and reversely.

Flare activity in cool stars is a very common phenomenon. Flares in stars with spectral type earlier than M are observed mainly in UV and X-rays and optical flares (like the most energetic white light flares in the Sun; Hudson et al., 2006) are rare. However, in the less luminous low mass dM stars optical flares often occur. It is also known, that red dwarfs from $\approx 0.3\,M_{\odot}$ down to the hydrogen burning limit can release a considerable amount of energy via flare eruptions, even when, in most cases, these objects show very low magnetic activity in their quiescent states.

The complete time-series data (obtained between 1999–2003) was used for the study of the detected flare. The object studied here, which has identifier M31 J00453912+4130395 in Chap. 2, was flagged during the course of the analysis as an object with a large brightening following the characteristic light curve shape of a stellar flare. The finding chart of the object, also cross-identified as 2MASS J00453912+4140395, is shown in Fig. A.1, which contains only a small portion of the full $33\farcm8 \times 33\farcm8$ WFC field of view. The B and V observations resulting from the DIA analysis and subsequent calibration to the standard system are plotted in Fig. A.2, where the large flare event (A) is zoomed in alongside of two other weaker flares (B, C).

A.2 Stellar properties

Table A.1 summarizes the quiescent B and V magnitudes from our INT data, as well as V and I magnitudes from the DIRECT catalog (Mochejska et al., 2001a), and J, H and K magnitudes from the 2MASS catalog (Skrutskie et al., 2006). A self-consistent analysis using the observed object color indexes and the extinction law of Drimmel et al. (2003) indicates a color excess of $E(B-V) = 0.05$ mag, and, adopting a ratio of 3.1 between A_V and $E(B-V)$, leads to an absolute extinction of 0.16 mag. The unreddened color indexes are most compatible with a spectral type M4 dwarf with $M_V = 13.8$ mag, $\log L/L_{\odot} \approx -2.5$, $\mathcal{M} \approx 0.16$ M$_{\odot}$ and $R \approx 0.2$ R$_{\odot}$ according to the tabulations from Baraffe & Chabrier (1996), Baraffe et al. (1998), and Bessell et al. (1998). The distance resulting from the analysis is of roughly 300 pc.

KPNO plates taken from the M 31 field (NOAO Science Archive, Aladin Sky Atlas[1]) also agree with a mid-M or later spectral type classification since the object

[1] http://aladin.u-strasbg.fr/

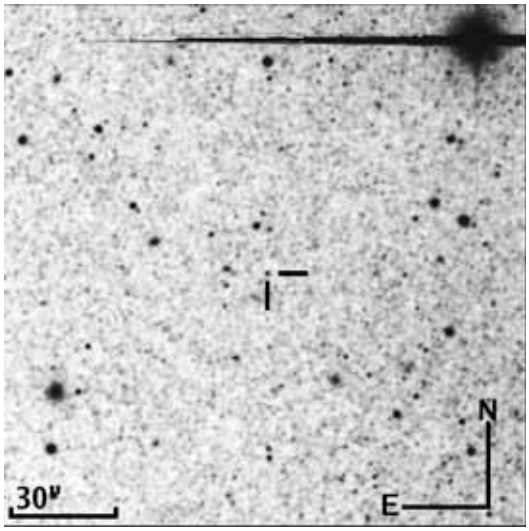

Figure A.1. Finding chart from the M 31 field with flare source (INT WFC image).

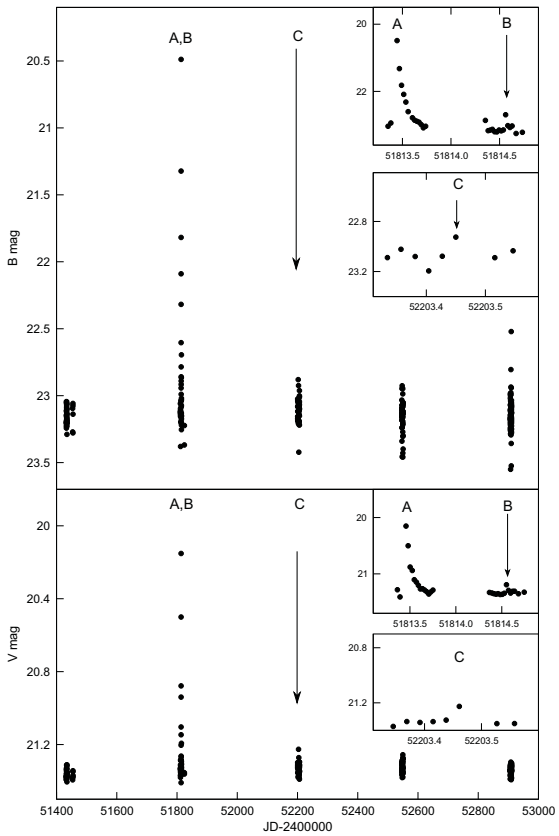

Figure A.2. Light curves in Johnson *B* and *V* of 2MASS J00453912+4140395, taken with the WFC of INT in La Palma, between 1999-2003. Three individual flare events (flares A, B and C) are marked and zoomed.

Table A.1. Catalog data on the observed target.

	INT WFC	DIRECT	2MASS
object ID	M31_J00453912+4140395	D31J004539.1+414039.5	J00453911+4140396
α (J2000)	00 45 39.12	00 45 39.11	00 45 39.12
δ (J2000)	+41 40 39.5	+41 40 39.46	+41 40 39.7
B	23.18		
σ_B	0.11		
V	21.38	21.62	
σ_V	0.03	0.07	
I		18.18	
σ_I		0.07	
J			16.35
σ_J			0.11
H			15.98
σ_H			0.16
K			15.63
σ_K			0.18

is best seen in the I-band KPNO plates, but also observable in Hα and R. However, in the U, B, and V band plates our target is indistinguishable from the background.

A first step towards evaluating the level of magnetic activity of the studied target is to investigate possible cyclic (rotational) variability induced by surface inhomogeneities (e.g., cool spots). No convincing sign of such modulation was found from our Fourier analysis. Three possible explanations can be put forward. First, spot coverage could be too small to observe any rotational modulation (this is the case when observing our Sun as a star in optical photometric bands). Alternatively, the star could be heavily spotted and yet show small or no modulation if spots are evenly distributed. If we compare the mean error of the measurements in B is 0.08 mag with a scatter of 0.11 mag, i.e., there is still room for some low-level modulation, although the V band does not seem to show such behavior with a scatter of 0.03 mag and a 0.04 mag formal error. The third possible scenario is a low inclination ($i \approx 0°$) of the rotation axis making it not possible to observe any rotational variability. However, in this latter case one could expect variability on a longer timescale of a few years, because of changes in the overall spot coverage according to solar-like spot activity cycle (see e.g. Oláh et al., 2000). No such long-term modulation is seen during the 5-year long observing season and 2MASS J00453912+4140395 seems to be like the vast majority of cool M dwarfs with rotational variability less than 1 – 2% in the visible.

A.3 Flare energy estimation

Flare statistics of red dwarf stars show that stellar flares can generally be divided into two subgroups: a group consisting of relatively small, shorter ($\approx 10^3$ s) im-

pulsive flares, and a more energetic group releasing at least 10^{32} erg and lasting $\approx 10^4$ s. The latter are often related to solar two-ribbon flares which are associated to filament eruptions and coronal mass ejections (CMEs). The basic properties of flare A observed on 2000 September 25 (beginning at HJD 2451813.45), such as the long duration reaching $\Delta t_B \approx 3 \times 10^4$ sec and the large amplitudes of ΔB =2.69 mag and $\Delta V = 1.23$ mag clearly class this event among the more energetic group.

Flare light curves usually consist of a rapid rise followed by a slower, monotonic decay. However, our poorly covered rising phase permits only a rough estimation of the physical properties. For the estimation of the flare energy first we derived intensity from the magnitude values:

$$\frac{I_{0+f}}{I_0} = 10^{\frac{\Delta m_{B,V}}{2.5}}, \tag{A.1}$$

where I_{0+f} and I_0 are the intensity values of the flaring and the quiescent stellar surfaces, respectively, in one of the observed bands. The relative flare energy is then obtained by integrating the flare intensity over the flare duration:

$$\mathcal{E}_f = \int_{t_1}^{t_2} (\frac{I_{0+f}(t)}{I_0} - 1)dt. \tag{A.2}$$

The quiescent stellar fluxes in different bands are estimated assuming a simple black body energy distribution for a dM4 star with $T_{\rm eff} = 3100\,$K, taking $R \approx 0.2R_\odot$ (see Sect. A.2) from the equation

$$F_\star = \int_{\lambda_1}^{\lambda_2} 4\pi R^2 \mathcal{F}(\lambda)\, S_{B,V}(\lambda) d\lambda, \tag{A.3}$$

where $\mathcal{F}(\lambda)$ is the power function and $S_{B,V}(\lambda)$ is the transmission function for a given passband. Finally, the total integrated flare energy is calculated by multiplying the relative flare energy and the quiescent stellar flux:

$$E_f = \mathcal{E}_f F_\star. \tag{A.4}$$

Since our flare light curve is poorly covered, the abrupt rising phase with its real peak value may be estimated as even 1.5 – 2 mag brighter in B and ≈1.3 mag brighter in V than the measured maxima. This assumption corresponds to a photometric flare temperature of $\approx 1.5 \times 10^4$ K at peak (cf., e.g., Ishida, 1990; Ishida et al., 1991, and references therein). According to this, the observed and dereddened $B - V$ peak of 0.29 mag is just an upper limit of a more reliable $B - V \approx -0.16$ mag. Calculated luminosities for the quiescent star, and the total flare energy for both the minimum fit and the more realistic assumption are summarized in Table A.2, together with the ratio of the flare energy and the quiescent

Table A.2. Quiescent stellar flux and flare energy estimations. A minimum flare energy is estimated both from a minimum fit of the observed data and also by a (more realistic) reconstruction of the rising phase (values in parenthesis).

band	quiescent flux 10^{29} [erg/s]	flare energy 10^{34} [erg]	equivalent duration [h]
B	5.09	3.56 (6.34)	19.4 (34.6)
V	12.76	1.77 (3.47)	3.9 (7.6)

stellar luminosity, often called as equivalent flare duration, i.e., the time interval in which the star would radiate as much energy as the flare itself. The ratio between the flare energies $E_B/E_V = 2.01$ (or 1.83 for the more realistic estimation) is in the order of the statistical value of $1.60^{+0.13}_{-0.32}$ from Lacy et al. (1976). Using the empirical correlation of

$$E_U = 1.2 \pm 0.08 E_B \tag{A.5}$$

we derive an estimation of 4.27 (7.61) 10^{34} erg for E_U. From this we can estimate the total flare energy released in the optical range as being in the order of a few times 10^{35} erg, and resulting in a value of $\simeq 10^{36}$ erg for the bolometric flare energy (cf. the review of Pettersen, 1989). This rough but still realistic estimation (cf. the example in Pagano et al., 1997, with $\sim$ 3 times more brightness in *U*) indicates that the 2000 September 25 flare is among the most energetic stellar flares ever observed.

A.4 Weak flaring and post-flare events

There are statistical evidences that flare-like transient phenomena, often called microflares, are almost continuously present on M-type dwarfs. These events are thought to be one of the major sources of chromospheric and coronal heating. We see them (sometimes as nanoflares) also on the Sun (e.g., Lin et al., 1984), however, because of being relatively weak and short-term events most of them remain unresolved.

For filtering out such short-duration events from the background of our photometric data we searched for small amplitude peaks occurred simultaneously in both photometric colors. We applied different filtering algorithms but finally a visual inspection proved to be the most reliable and efficient. Two such events are apparent. One is just one day after flare A at HJD 2451814.55 (marked with B in Fig. A.2) and another one at HJD 2452203.45 (flare C in Fig. A.2). There are some additional albeit less convincing ones, which are only 2-σ away from the photometric background, and therefore were disregarded. Following the method described in Sect. A.3 we estimate the total energy of flares B and C to be from

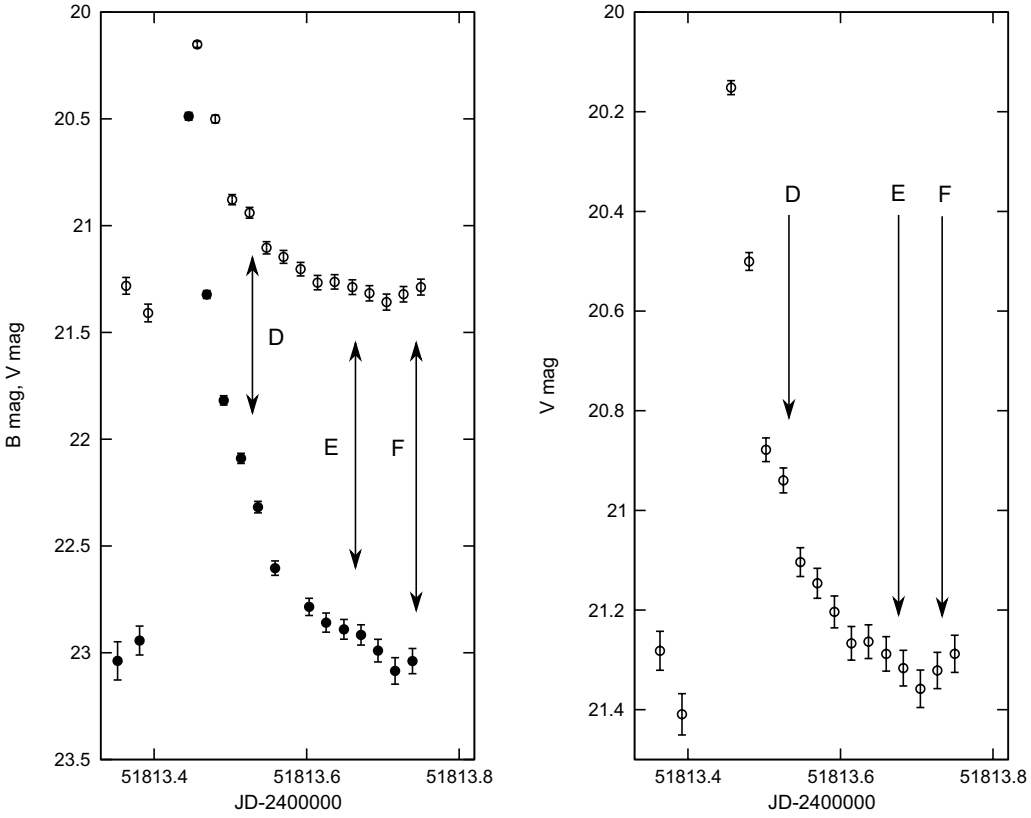

Figure A.3. The large flare of 2000 September 25 (flare A in Fig. A.2) with three post-flare events (D,E and F). *Left.* *B* (dots) and *V* (circles) light curves together. **Right:** Zoomed *V* curve plotted alone.

a few times 10^{32} erg up to 10^{33} erg in *B*, which are characteristic of a short-term impulsive flares rather than microflares.

When analyzing the decay phase of the light curve of flare A, three other short term increases can be identified. Since those events occurred simultaneously in both colors, we assume them to be an additional three weak flares: one at HJD 2451813.54 (D in Fig.A.3), another one at HJD 2451813.67 (E) and a third one just at the end of the large flare light curve at HJD 2451813.74 (F), all of them lasting about $\Delta t \approx 8 \times 10^3$ sec (in the case of flare F, the simultaneous rise in *B* and *V* together is considered as just the beginning of the flare event and its duration is extrapolated). Again, we estimate the total flare energies as $2 - 6 \times 10^{31}$ erg in *B* and about a half of this value in *V*. The occurrence of such weak post-flare events in the descending phase of a large long duration flare is a reminder of the mechanism described first by Attrill et al. (2007), which probably occurs on the Sun during large CMEs. After energetic solar flares are associated with CMEs, the moving footpoints of the blowing up magnetic loop crosstalk with opposite polarity flux ropes from the randomly distributed magnetic carpet, or other favorably oriented magnetic concentrations (active regions), thus forming

current sheets and triggering other (micro)flare events from time to time. This seems a plausible interpretation for the three weak flare-like events (D, E and F) observed during the decay phase of flare A.